

Assessment of Electric Power and Refrigeration Production by Using Solar Thermal Energy for Industrial Applications

Guillermo Martínez-Rodríguez^{a,*}, Juan-Carlos Baltazar^b, Amanda L. Fuentes-Silva^a

^aDepartment of Chemical Engineering, University of Guanajuato, Noria Alta s/n, 36050, Guanajuato, MEXICO.

^bEnergy Systems Laboratory, TEES, 7607 Eastmark Drive, College Station, TX 77840, USA

corresponding.author: guimarod@ugto.mx

Solar thermal energy can supply the total or partial thermal load in low-temperature industrial processes. In industry, applications of solar thermal energy may extend to produce electric power and refrigeration in a viable way. This work proposes a solar system composed by a storage system, low-temperature solar collector field, an organic Rankine cycle, and an absorption refrigeration system (Water/Lithium Bromide) to produce electric power and refrigeration. To evaluate the system performance, and its thermal and economic feasibility, an analysis, both in a continuous process and in a batch process, of a food industry was conducting. By this way, was possible to find operating conditions based on competitive cost of energy and decreasing CO₂ emissions. An absorption refrigeration system with a thermal load value of 176 kW, and a thermal performance coefficient (COP) of 0.87, had a thermal solar energy levelized cost (LCOE_{th}) of 0.0588 USD per kWh. ORC electric energy (LCOE_{ele}) had a charge of 0.1089 USD per kWh and a thermal efficiency of 0.11. Energy costs in kWh showed to be competitive, since they are in the order of the prices of conventional sources of energy, additionally, the emissions can reduce to zero.

1. Introduction

Solar energy experimented an extraordinary worldwide capacity expansion in 2020, majorly in China; with 127 GW (+22 %) close to wind energy (capacity expansion: 111 GW, +18 %). These numbers make up 91 % of all renewable energy expansions in 2020 (IRENA, 2021). Showing the interest and global commitment to beat down climate change. According to the Annual Energy Outlook 2022 (EIA, 2022), renewables power generation was 21 % in 2021, mostly by solar and wind energy. Nevertheless, 2021 will be also known as the year in which CO₂ emissions reached the highest level regarded 2010. A rise by 6 % compared 2020 (36,3 gigatons) generated by electricity and heat production because the necessity to complement the energy demand with fossil fuels (IEA, 2022). A growing industry in the world is that of food products. One of them is the dairy industry, which, in USA, supplied between 2008 and 2012, around 2 % of total country GHG emissions (U.S. Dairy's 2013.). Since the last two decades (Benz et al., 1998), innovations in the processes of the dairy industry have transformed the sector to now be an area of good environmental practices. Combined solar heat refrigeration and power (CHRP) or trigeneration (Bellos and Tzivandis, 2018), combined solar heat and power (CHP) or cogeneration, hybrid renewable energy systems (HRES) (Come et al., 2021), simultaneous production of heat and power (Martínez-Rodríguez et al., 2021), solar thermal water and photovoltaics-based pumping systems (Solanki & Pal, 2021) are among the main efforts to reduce the ecological footprint of dairy, and in general, of food industry, which mainly manages low-temperature processes (60 to 120 °C) to concentrate, evaporate, pressurize, pasteurize, clean, boil feed water, pre-heat, wash, refrigerate (Kalogirou, 2003). To integrate solar energy in a manufacturing or chemical process, it is necessary to perform a deep analysis of its operation details and pre-existing heat supplies, to set the different temperature levels of the process and the possible energy savings and, in this way, achieve the maximum use of energy with the consequent economic and environmental impacts. For this, multiple objectives must be established a priori, like solar fraction, environmental, economic, and technical, to name some (Martínez-Rodríguez et al., 2022).

Production of electricity from photovoltaic solar cells is the most common way, although this is also possible from solar thermal energy by means of a power cycle like organic Rankine cycle (ORC) which functions with

low temperature. Furthermore, refrigeration can be achieved from solar energy. Today, solar absorption refrigeration system that uses water and lithium bromide or water and ammonia as refrigerants, is being widely studied because is a less harmful alternative to the environment, compared with traditional vapor compression refrigeration and requires low temperature to work, although it is needed to improve its low COP (coefficient of performance) (Dhindsa, 2021).

Taking into consideration all this background, in the current research was demonstrated the feasibility of a 100 % renewable energy system to produce the power and refrigeration of a cold room through solar thermal energy, generating zero net emissions of greenhouse gases and a competitive energy cost estimated at 0.2042 USD/kWh.

2. Design of the energy system to produce power and refrigeration

Figure 1 is a diagram of the energy system proposed to produce the power and cooling required by the process by harnessing solar thermal energy. The aim is for the energy system to be total renewable. The main components of the proposed energy system are a low-temperature solar thermal facility (network of solar collectors and thermal storage system) that provides the heat load to operate an organic Rankine cycle and an absorption refrigeration cycle. Initially, is conducted a thermodynamic analysis of each component of the system to determine the variables that have the greatest impact on the design, to later assemble all the parts of an energy system. Among the most important considerations for the design of the energy system are these aspects: thermodynamic and/or operational, economic, and environmental.

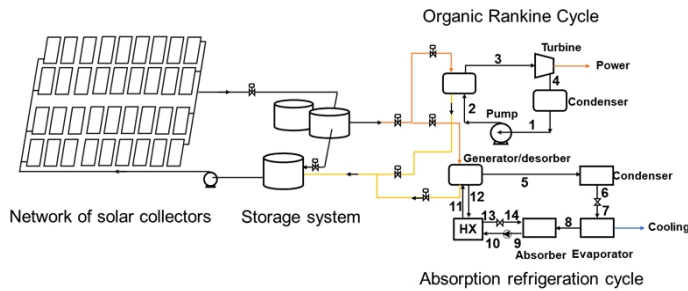


Figure 1: General diagram of the design of the proposed energy system to generate electrical energy and refrigeration.

2.1 Network of low temperature solar collectors

The network of low-temperature solar collectors was designed through the methodology proposed by Martínez-Rodríguez et al., (2019). The size and arrangement of the solar collector network were determined under the average irradiance conditions that occur in the winter period in the city of Guanajuato, Mexico. To guarantee the supply of the thermal load and the target temperature, the variation of daily radiation is considered in the number of collectors connected in series. For an irradiance level at a given time, the collectors connected in series guarantee the target temperature and the series connected in parallel guarantee the supply of the thermal load.

2.2 Energy storage system

The energy storage system represents 30 % of the cost of the solar thermal installation (Karagiorgas et al., 2001). The operation of this system is essential to store energy, cushion fluctuations in the variability of the solar resource, and increase the solar fraction of the process when there is a mismatch between energy production and demand. To determine the volume of the thermal storage system, V_{SAT} , the Eq(1) is used (Yang et al., 2014).

$$V_{SAT} = \frac{\dot{Q}_u \Delta t}{C_p \Delta T_{SAT} \rho} \quad (1)$$

Where, \dot{Q}_u is the total thermal load to be stored (kW), Δt is the energy storage time (h), C_p is the heat capacity of the working fluid (kJ/kg °C) and ρ is the density of the thermal fluid (kg/m³) and ΔT_{SAT} is the temperature variation of the thermal storage system (°C).

2.3 Organic Rankine cycle

The organic Rankine cycle is a mature technology that makes the best commercial solution available for electricity production (Authin et al., 2021). Organic Rankine cycle (ORC) systems show great potential for use in small-scale systems (<10 kWe) with low-temperature collectors (Freeman et al., 2017). Solar assisted low-temperature Rankine cycle for power generation consists of the following components: evaporator, turbine, condenser, and pump. The working fluid is pumped at high pressure by the feed pump, the high-pressure liquid is heated in the evaporator where the phase change occurs and is subsequently superheated. The generated steam produces power in a turbine, and the exhaust steam at the turbine outlet goes to the condenser, where that is condensed with cooling water and liquid refrigerant is pumped in to restart the cycle.

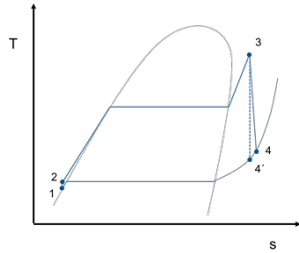


Figure 2: T-s diagram for the Rankine cycle.

The thermal load that the evaporator needs to produce steam is taken from the thermal storage system. The thermal load required by the evaporator, \dot{Q}_{E1} , to operate the Rankine cycle is calculated using the Eq(2).

$$\dot{Q}_{E1} = \dot{m}_{f1}(h_2 - h_3) \quad (2)$$

Where, \dot{m}_{f1} is the flow of the working fluid (kg/s), h_2 and h_3 are the enthalpies at the inlet and outlet of the evaporator, respectively (kJ/kg). An isentropic expansion of the working fluid vapor takes place in the turbine, which ideally is also reversible and adiabatic. The work produced isentropically by the turbine, W_{isen} , is given by the Eq(3).

$$W_{isen} = \dot{m}_{f1}(h_4 - h_3) \quad (3)$$

Which is defined by the change in the input and output enthalpies, h_4 and h_3 , of this device. Different literature sources establish that in conventional thermoelectric plants, steam turbines quantify the losses of availability of energy in the turbine at an average of 8 %. Therefore, the work produced by the turbine, W_T , is calculated as a function of the turbine efficiency using Eq(4).

$$W_T = \dot{m}_{f1}(h_4 - h_3)\eta_T \quad (4)$$

Where, η_T is the efficiency of the turbine-generator, with a value of 92 % and the efficiency of the generator, the efficiency of the pump, η_{P1} , is set to 85 %. The net electricity produced by the system, W_{Net} , is defined by Eq(5).

$$W_{Net} = W_T - W_{P1} \quad (5)$$

The calculation of the efficiency of the power cycle, η_{ORC} , establishes the relationship between the net electrical energy produced and the heat supplied in the evaporator, \dot{Q}_{E1} , given by Eq(6).

$$\eta_{ORC} = \frac{W_{Net}}{\dot{Q}_{E1}} \quad (6)$$

2.4 Single effect absorption refrigeration system

The difference between absorption and vapor compression systems is the method that is used to transport the refrigerant from the low-pressure region of the cycle to the high-pressure ones; since, instead of a compressor to perform said action, the absorption system uses a chemical process. The current research refers to an absorption refrigeration system powered by a solar energy system illustrated in Figure 1. The technology of flat solar collectors reaches a maximum operating temperature of 105 °C. The refrigeration device examined is a single-stage absorption chiller with an H₂O-LiBr absorbent pair. An absorption cycle is a refrigeration cycle that uses thermal compression to rise the water pressure and increases the pressure of H₂O, the effect produced is

like use a compressor. In the condenser, H₂O is a high-pressure saturated liquid at its outlet. On the evaporator, it must be indicated that its output is a low-pressure saturated steam.

The energy balance in each of the stages of the refrigeration cycle is shown below, starting at the evaporator stage given by Eq(7).

$$\dot{Q}_{E2} = \dot{m}_{f2}(h_8 - h_7) \quad (7)$$

Where, \dot{Q}_{E2} is the thermal load of the evaporator (kW), h_8 is the outlet stream enthalpy (kJ/kg), h_7 is the inlet stream enthalpy (kJ/kg) and \dot{m}_{f2} is the mass flow of refrigerant (kg/s). The next stage is the absorber, which relates the streams of high and low concentration of refrigerant established by Eq(8), where \dot{Q}_A is the thermal load of the absorber (kW), h_8 , h_{14} and h_9 are the enthalpies of the input streams and the output stream (kJ/kg), respectively, \dot{m}_8 , \dot{m}_{14} and \dot{m}_9 are the mass flow of streams (kg/s).

$$\dot{m}_8 h_8 + \dot{m}_{14} h_{14} = \dot{Q}_A + \dot{m}_9 h_9 \quad (8)$$

The Eq(9) is the energy balance in the generator (or desorber).

$$\dot{m}_{11} h_{11} + \dot{Q}_G = \dot{m}_7 h_7 + \dot{m}_5 h_5 \quad (9)$$

Where \dot{Q}_G is the heat load employed to separate the water (refrigerant) and the Lithium Bromide (absorber) to produce the required refrigeration by the process, in kW; h_{11} , h_7 and h_5 are the enthalpies of the inlet and outlet streams (kJ/kg), \dot{m}_{11} is the mass flow of the input stream to the generator, \dot{m}_7 and \dot{m}_5 are the mass flow of the output streams of this stage (kg/s). Eq(10) represents the energy balance in the condenser, \dot{Q}_C . Where h_5 is the enthalpy of the inlet stream and h_6 is the enthalpy of the output stream (kJ/kg), and \dot{m}_5 and \dot{m}_6 are the mass flow of these streams (kg/s).

$$\dot{m}_5 h_5 = \dot{Q}_C + \dot{m}_6 h_6 \quad (10)$$

The energy balance is complete considering the exchanger and the cycle pump, represented by Eq(11) and Eq(12), respectively.

$$\dot{m}_{12} h_{12} + \dot{m}_{10} h_{10} = \dot{m}_{11} h_{11} + \dot{m}_{13} h_{13} \quad (11)$$

$$W_{P2} = \frac{\dot{m}_2 (p_{10} - p_9)}{\gamma_{sln}} \quad (12)$$

The enthalpies of the exchanger inlet streams are h_{10} and h_{12} , and the enthalpies of the outlet streams are h_{11} and h_{13} (kJ/kg). The work done by the pump is W_{P2} (kW), p_{10} and p_9 are the outlet and inlet pressures at the pump (kPa), and γ_{sln} is the density of the mixture (m³/kg). Also, the pertinent considerations for the sizing of the valves are made. Finally, the material balance is made at each stage. To evaluate the thermal efficiency of the refrigeration cycle, the COP (Coefficient of Performance) given by Eq(13) is evaluated, which relates the amount of energy supplied to the generator, \dot{Q}_G , with the kW obtained in the evaporator, \dot{Q}_E .

$$COP = \frac{\dot{Q}_E}{\dot{Q}_G + W_{P2}} \quad (13)$$

2.5 Energy cost estimation

The levelized cost of energy, LCOE, is an indicator adopted for the evaluation of the profitability of these systems, meanwhile, it also helps to compare the production of power systems. The LCOE relates the cost for each unit of energy produced, in USD /kWh, defined by Eq(14).

$$LCOE = \frac{CFR \cdot C_{inv} + C_{op\&maint} + C_{fuel}}{\dot{W}_{net} \cdot Hours} \quad (14)$$

In estimating the cost of energy, the capital cost of the main components is considered, as well as the costs of infrastructure, maintenance, supervision, auxiliary services, among others. The life span of the plant is 25 years, the interest rate of the project is taken as 8 % and the prices are adjusted for the year 2021.

3. Case study: fruit and vegetable cold room

A cooling room to preserve fruits operates 24 h/day during 360 days per year. Energy demand by year is 1.52 GWh for refrigeration and 294 MWh for electric power. The cooling room stores per year 1,800 t of apples and

850 t of potatoes, at temperatures between 5 to 10 °C. The energy system proposed is based on solar thermal energy use to refrigerate and feed electric power as required by the process; a solar collector network and a solar storage system meet the demand of an absorption refrigeration cycle and an organic Rankine cycle, ORC.

4. Results

Figure 3 shows the relationship between variables that have a greater impact on the efficiency of the ORC and the performance of the refrigeration cycle. Figure 3a shows the graph of the relationship between ORC efficiency and turbine feed temperature for two refrigerants, R245fa and R12. Figure 3b shows the effect of the solution refrigerant concentration on the COP for different operating temperatures in the evaporator (TE). Considering that solar thermal temperature is supplied at 105 °C, the efficiency of the ORC is between 0.08 and 0.15. And, for the absorption refrigeration system, the concentration of the strong solution has a greater influence on the performance of the cycle, with a COP between 0.67 and 0.87.

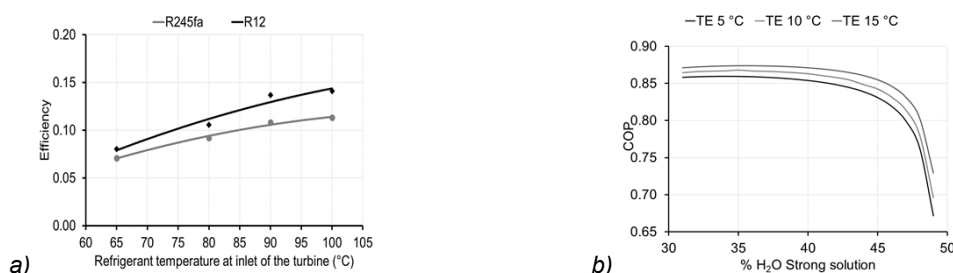


Figure 3: Relationship between variables of the power and refrigeration cycles.

Table 1 shows the results obtained for the energy system designed to supply electrical energy and the refrigeration service of the cold room using solar energy entirely, that is, the solar fraction is 1. The emissions that are no longer released into the atmosphere are 378 t of CO₂/year with a total energy cost of 0.2042 USD/kWh.

Table 1: Design parameters for solar thermal facility and refrigeration system.

<i>Design parameters of the solar thermal installation</i>	
Solar thermal system temperature, °C	105
Arrangement of the solar collector network (parallel-series)	68x29
Solar collector network size, m ²	3609
Thermal storage system volume, m ³	55
Levelized cost of energy (solar thermal), USD/kWh	0.0365
<i>Design parameters for the ORC R245fa</i>	
Electrical power output, kWh/day	816
Refrigerant temperature at the inlet of the turbine, °C	90
Power cycle efficiency	0.11
Levelized cost of energy (electrical), USD/kWh	0.1089
<i>Design parameters for the single effect H₂O-LiBr absorption</i>	
Refrigeration power, kW	176
Strong solution temperature at desorber, °C	90
Refrigerant temperature at the inlet of the evaporator, °C	5
Refrigeration cycle performance	0.87
Levelized cost of energy (refrigeration), USD/kWh	0.0588

5. Conclusions

The best performance of the refrigeration system, COP of 0.87, is achieved at 90 °C in the absorber, which maintains a temperature of 5 °C in the cold room.

The concentration of the refrigerant (strong solution) influences in a significant way the performance of the refrigeration cycle. The best COP was reached with a strong solution concentration of 35 %.

Thermal efficiency of the ORC was 0.11, employing low temperature solar collectors. With this efficiency, the cost of kWh_{ele} is 0.1089 USD, which is competitive compared to the cost of kWh produced by means fossil fuels. Energy cost of the proposed fully renewable energy system was estimated at 0.2042 USD/kWh compared to the price of electricity reported for Mexico during 2021, 0.1670 USD/kWh, observing a difference of 22 %. It is feasible to implement at an industrial level the use of low-temperature solar thermal energy for refrigeration and energy. However, the impact on the environment, damage to health and social development are not evaluated in the cost of energy using fossil fuels and renewable energies, in addition to the fact that large subsidies for several economic sectors are given.

Acknowledgements

The authors thank the support of Ms. Evangelina Sánchez-García on synthesizing on-line literature.

References

- Authin E.A., Liew P.Y., Klemeš J.J., Ho W.S., Che Jusoh N.W., Mohammad Rozali N.E., 2021. Integration of Combined Heat and Power Energy Systems with Gas Turbine in Locally Integrated Energy Sectors. *Chemical Engineering Transactions*, 83, 37-42.
- Bellos E., Tzivandis C., 2018, Evaluation of a solar driven trigeneration system with conventional and new criteria, *International Journal of Sustainable Energy*, DOI: 10.1080/14786451.2018.1494173.
- Benz N., Gut M., Rub W. (1998) Solar process heat in breweries and dairies. In: *Proceedings of EuroSun 98*. Portoroz, Slovenia.
- Come E.I., van der Windt H., Nhumaio G., Faaij A.P.C., 2021, A review of hybrid renewable energy systems in mini-grids for off-grid electrification in developing countries, *Renewable and Sustainable Energy Reviews*, 144, 111036. doi:10.1016/j.rser.2021.111036.
- Dhindsa G.S., 2021, Review on performance enhancement of solar absorption refrigeration system using various designs and phase change materials, *Materials Today: Proceedings*, 37, 3332-3337. doi: 10.1016/j.matpr.2020.09.125
- EIA AEO, 2022, Annual Energy Outlook 2022, U. S. Energy Information Administration <<https://www.eia.gov/todayinenergy/detail.php?id=51698>> accessed 04.04.2022.
- Freeman J., Guarracino I., Kalogirou S.A., Markides C.N., 2017. A small-scale solar organic Rankine cycle combined heat and power system with integrated thermal energy storage. *Applied Thermal Engineering*, 127, 1543-1554. doi:10.1016/j.applthermaleng.2017.07.163
- IEA Global Energy Review: CO₂ Emissions in 2021, March 2022, US International Energy Agency, <<https://www.iea.org/reports/global-energy-review-co2-emissions-in-2021-2>> accessed 02.04.2022.
- IRENA, Renewable Capacity Statistics 2021, March 2021, International Renewable Energy Agency, <<https://www.irena.org/publications/2021/March/Renewable-Capacity-Statistics-2021>> accessed 02.04.2022.
- Kalogirou S., 2003, The potential of solar industrial process heat applications, *Applied Energy*, 76, 337-361. doi: 10.1016/S0306-2619(02)00176-9.
- Karagiorgas M., Botzios A., Tsoutsos, T., 2001, Industrial solar thermal applications in Greece Economic evaluation, quality requirements and case studies, *Renewable and Sustainable Energy Reviews*, 5, 157–173. doi: 10.1016/s1364-0321(00)00012-5
- Martínez-Rodríguez G., Fuentes-Silva A.L., Lizárraga-Morazán J.R., Picón-Núñez M., 2019, Incorporating the Concept of Flexible Operation in the Design of Solar Collector Fields for Industrial Applications, *Energies*, 12, 570. doi:10.3390/en12030570
- Martínez-Rodríguez G., Fuentes-Silva A.L., Baltazar J.-C., 2021, Simultaneous Production of Solar Thermal Heat and Power for Industrial Applications, *Chemical Engineering Transactions*, 88, 505-510, DOI:10.3303/CET2188084.
- Martínez-Rodríguez, Baltazar J.-C., Fuentes-Silva A.L., García-Gutiérrez R., 2022, Economic and Environmental Assessment Using Two Renewable Sources of Energy to Produce Heat and Power for Industrial Applications, *Energies*, 15, 2338. doi:10.3390/en150723382022.
- Solanki A., Pal Y., 2021, Comprehensive review to study and implement solar energy in dairy industries, *Journal of Thermal Engineering*, 7, 1 216–1238. 10.18186/thermal.978029
- U.S. Dairy's Environmental Footprint. A summary of findings 2008-2012, 2013, Innovation Center for US Dairy, <<https://www.usdairy.com/getmedia/42a3aeae-381e-48ba-bb91-a5fca1b77e0b/dairysenvironmentalfootprintpdf.pdf.aspx>> accessed 02.04.2022.
- Yang P., Liu L.L., Du J., Li J.L., Meng Q.W., 2014, Heat exchanger network synthesis for batch processes by involving heat storages with cost targets, *Applied Thermal Engineering*, 70, 1276–1282. doi:10.1016/j.applthermaleng.2014.05.041